Proceedings of the XIII National School of Superconductivity, Lądek Zdrój 2007

d-Wave Superconductivity, Orbital Magnetism, and Unidirectional Charge Order in the *t*–*J* Model

M. Raczkowski

Marian Smoluchowski Institute of Physics, Jagiellonian University
Reymonta 4, PL-30-059 Kraków, Poland

Recent scanning tunneling microscopy in the superconducting regime of two different cuprate families revealed unidirectional bond-centered modulation in the local electronic density of states. Motivated by this result we investigate the emergence of modulated d-wave superconductivity coexisting with charge domains that form along one of the crystal axes. While detailed stripe profiles depend on the used form of the Gutzwiller factors, the tendency towards a valence bond crystal remains robust. We also find closely related stripe phase originating from the staggered flux phase, a candidate for the pseudogap phase of lightly doped cuprates.

PACS numbers: 74.72.−h, 74.20.Mn, 74.81.−g, 75.40.Mg

1. Introduction

It is now well established that the simplest model proposed to describe the physics of the high-T_c superconductors, the so-called t–J model [1],

$$\mathcal{H} = -t \sum_{\langle ij\rangle,\sigma} (\tilde{c}^{\dagger}_{i\sigma}\tilde{c}_{j\sigma} + \text{h.c.}) + J \sum_{\langle ij\rangle} \boldsymbol{S}_i \cdot \boldsymbol{S}_j, \tag{1}$$

where $\tilde{c}^{\dagger}_{i\sigma} = (1 - n_{i,-\sigma})c^{\dagger}_{i\sigma}$ is the Gutzwiller projected electron operator and $n_{i\sigma}$ is the particle number operator, yields apart from the true long-range magnetic order, characteristic of the undoped parent Mott insulators, an array of quantum SU(2)-invariant ground states [2]. In fact, it is quite natural to expect that strong quantum fluctuations arising from both low spin $S = 1/2$ of the copper ions and the two-dimensional nature of the CuO_2 planes, should lead to *quantum disordered* states with only short-range antiferromagnetic (AF) spin correlations. The most famous example of such states is a resonating valence bond (RVB) phase [3]. Remarkably, Anderson's RVB theory based on a Gutzwiller projected BCS trial wave function, whose parameters are usually determined either by using renormalized mean field theory (RMFT) [4] or by variational Monte Carlo (VMC) method [5],

not only predicted correctly the d-wave symmetry of the superconducting (SC) order parameter [6], but in addition, it reproduced experimental doping dependence of a variety of physical observables in the SC regime [7].

Moreover, the tendency towards valence bond amplitude maximization might enhance charge and spin stripe correlations in the d-wave RVB state. The presence of charge and long-range spin stripe order has been detected in neutron scaterring experiments and confirmed in resonance X-ray scattering in a few special cuprate compounds, namely $La_{1.6-x}Nd_{0.4}Sr_xCuO_4$ and $La_{2-x}Ba_xCuO_4$ [8]. However, such stripe order competes with superconductivity and thus strongly reduces T_c [9]. In contrast, recent scanning tunneling microscopy (STM) on different cuprate families $Ca_{2-x}Na_xCuO_2Cl_2$ and $Bi_2Sr_2Dy_{0.2}Ca_{0.8}Cu_2O_{8+\delta}$, has revealed intense spatial variations in asymmetry of electron tunneling currents with bias voltage that forms unidirectional domains coexisting with inhomogeneous d-wave superconductivity [10]. In particular, it has been found that the asymmetry occurs primarily at the oxygen sites being indicative of a short-range *bond-centered* charge pattern with a period of four lattice spacings. In this paper we show that the bond-centered modulation observed in the STM experiments might be naturally interpreted in terms of a valence bond crystal, i.e., spin-rotationally invariant phase with spatially varying bond charge hopping and a concomitant modulation of short-range AF correlations [11].

2. Renormalized mean-field theory

We begin by discussing RMFT of the t–J model applied to the case with homogeneous charge distribution. In this approach, the Gutzwiller projection removing double occupancy is handled with statistical weight factors $g_t = 2x/(1+x)$ and $g_J = 4/(1+x)^2$ which account for different probabilities of hopping and superexchange processes in the projected and unprojected wave functions. Hence the mean-field Hamiltonian reads,

$$H = -t \sum_{\langle ij\rangle,\sigma} g_{ij}^t (c_{i,\sigma}^\dagger c_{j,\sigma} + \text{h.c.}) - \mu \sum_{i,\sigma} n_{i,\sigma}$$
$$-\frac{3}{4} J \sum_{\langle ij\rangle,\sigma} g_{ij}^J [(\chi_{ji} c_{i,\sigma}^\dagger c_{j,\sigma} + \Delta_{ji} c_{i,\sigma}^\dagger c_{j,-\sigma}^\dagger + \text{h.c.}) - |\chi_{ij}|^2 - |\Delta_{ij}|^2], \qquad (2)$$

with the Bogoliubov–de Gennes self-consistency conditions for the bond- $\chi_{ji} = \langle c_{j,\sigma}^\dagger c_{i,\sigma}\rangle$ and pair-order $\Delta_{ji} = \langle c_{j,-\sigma} c_{i,\sigma}\rangle = \langle c_{i,-\sigma} c_{j,\sigma}\rangle$ parameters in the unprojected state. Hereafter, we shall assume a typical value $t/J = 3$.

Even though the original proposal for the high-T_c superconductivity was the s-wave BCS wave function, it immediately turned out that it is the d-wave BCS state with $\Delta_{ij} = \pm\Delta$ for the nearest-neighbor pairs along the x (y) axis, respectively, which gives the lowest energy [6]. At half-filling, such a phase is equivalent to the staggered flux (SF) state with complex $\chi_{ij} = \chi \exp((-1)^{i_x+j_y} i\phi)$ yielding circulating currents whose chirality alternates from plaquette to plaquette [12]. In this limit, the t–J model reduces to the Heisenberg Hamiltonian with the local

SU(2) gauge symmetry corresponding to the following particle–hole transformation:

$$\begin{pmatrix} c_{i\uparrow}^{\dagger} \\ c_{i\downarrow} \end{pmatrix} = \begin{pmatrix} \alpha_i & \beta_i \\ -\beta_i^{*} & \alpha_i^{*} \end{pmatrix} \begin{pmatrix} c_{i\uparrow}^{\dagger} \\ c_{i\downarrow} \end{pmatrix}, \tag{3}$$

with $\alpha_i\alpha_i^{*} + \beta_i\beta_i^{*} = 1$. It mixes an $\uparrow$-spin particle with a $\downarrow$-spin hole and hence decouplings in terms of Δ or χ become indeed equivalent. In order to appreciate this better let us consider the related Hamiltonian matrices using the Bogoliubov–Nambu formalism with $\eta_{\boldsymbol{k}} = (c_{\boldsymbol{k}\uparrow}, c_{-\boldsymbol{k}\downarrow}^{\dagger})$ for the d-wave RVB phase and $\eta_{\boldsymbol{k}} = (c_{\boldsymbol{k},\sigma}, c_{\boldsymbol{k}+\boldsymbol{Q},\sigma})$ with $\boldsymbol{Q} = (\pi,\pi)$ for the SF phase

$$M_{\boldsymbol{k}}^{\mathrm{RVB}} = \begin{pmatrix} -\varepsilon_{\boldsymbol{k}} - \mu & \Delta_{\boldsymbol{k}} \\ \Delta_{\boldsymbol{k}} & \varepsilon_{\boldsymbol{k}} + \mu \end{pmatrix}, \qquad M_{\boldsymbol{k}}^{\mathrm{SF}} = \begin{pmatrix} -\varepsilon_{\boldsymbol{k}} - \mu & \mathrm{i}\chi_{\boldsymbol{k}} \\ -\mathrm{i}\chi_{\boldsymbol{k}} & \varepsilon_{\boldsymbol{k}} - \mu \end{pmatrix}, \tag{4}$$

where $\varepsilon_{\boldsymbol{k}} = (tg^{t} + \frac{3}{4}Jg^{J}\mathrm{Re}\chi)\gamma_{+}$, $\Delta_{\boldsymbol{k}} = \frac{3}{4}Jg^{J}\Delta\gamma_{-}$, $\chi_{\boldsymbol{k}} = \frac{3}{4}Jg^{J}\mathrm{Im}\chi\gamma_{-}$ with $\gamma_{\pm} = 2(\cos k_x \pm \cos k_y)$. Therefore, the corresponding spectra are given by

$$E_{\boldsymbol{k}}^{\mathrm{RVB}} = \pm\sqrt{(\varepsilon_{\boldsymbol{k}} - \mu)^2 + \Delta_{\boldsymbol{k}}^2}, \qquad \text{and} \qquad E_{\boldsymbol{k}}^{\mathrm{SF}} = -\mu \pm \sqrt{\varepsilon_{\boldsymbol{k}}^2 + \chi_{\boldsymbol{k}}^2}.$$

At half-filling ($\mu = 0$), one finds $\Delta = \chi = 0.169$ ($\chi = 0.239$ and $\phi = \pi/4$) for the d-wave RVB (SF) phase, respectively. Hence, in the latter case $\mathrm{Re}\chi = \mathrm{Im}\chi = 0.169$ and, since $\Delta_{\boldsymbol{k}} = \chi_{\boldsymbol{k}}$, both spectra become degenerate. As shown in Fig. 1a, the key feature of the obtained spectrum is that the energy gap vanishes linearly along the $S = (\pi/2, \pi/2)$ point forming a cone-like dispersion. While this cone remains pinned to the Fermi surface in the d-wave RVB phase, finite doping takes the node of the SF order away from the Fermi surface and opens hole pockets around the S point (see Fig. 1b,c). Nevertheless, both excitation spectra remain similar, which makes the SF phase an excellent candidate for the normal pseudogap phase that emerges below a characteristic temperature T^{*}. Moreover, short-range staggered orbital current–current correlations have been found in the Gutzwiller-projected d-wave RVB phase [13], in the exact ground state of the t–J model with a negative two-hole binding energy [14], as well as by analyzing motion of a hole pair in the AF background [15].

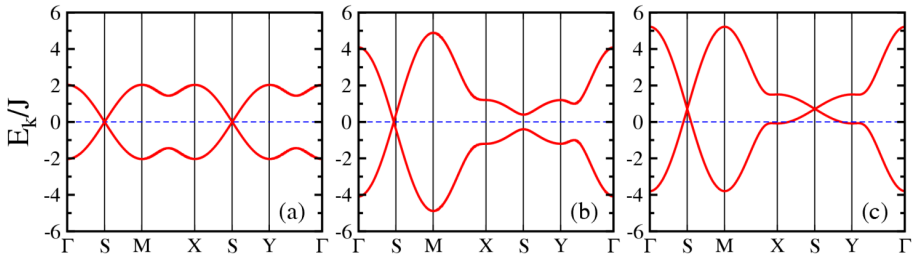

Fig. 1. Electronic structure along the main directions of the Brillouin zone of: (a) d-wave RVB/SF ($x = 0$); (b) d-wave RVB and (c) SF phase (both for $x = 1/8$).

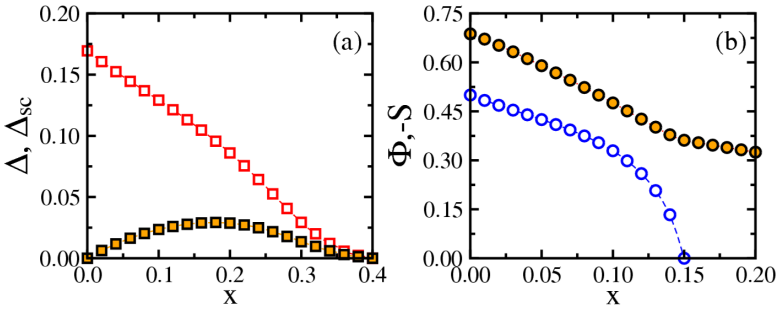

Fig. 2. Doping dependence of: (a) pairing amplitude Δ (open squares) and SC order parameter $\Delta_{\rm SC}$ (solid squares) in the d-wave RVB phase, as well as (b) plaquette flux Φ (open circles) and spin correlations $\mathcal{S}$ (solid circles) in the SF phase.

Next, as shown in Fig. 2a, variational parameter Δ is the largest at $x = 0$ and vanishes linearly with doping. In contrast, g^t is an increasing function of x so that the resulting SC order parameter $\Delta_{\rm SC} = g^t\Delta$ reproduces qualitatively the SC dome. Finally, Fig. 2b depicts the doping dependence of the fictitious flux (in unit of the flux quantum) defined by a sum over the four bonds of the plaquette $\Phi_{\square} = \frac{1}{2\pi}\sum_{\langle ij\rangle\in\square}\Theta_{ij}$ as well as the AF spin correlations $\mathcal{S} = -\frac{3}{2}g^J|\chi|^2$. Here, the appearance of a finite flux at $x \approx 0.15$ clearly strengthens $\mathcal{S}$ with respect to the Fermi liquid state where χ is entirely real.

3. Unidirectional charge order

We turn now to the discussion of bond-centered (with a maximum of the hole density spread over two-leg ladders) inhomogeneous RVB (chiral) states derived from the parent d-wave RVB (SF) phases, respectively. Hereafter we refer to the former as π-phase domain RVB phase (πDRVB), as it involves two out-of-phase SC domains (see also Ref. [16]), separated by horizontal bonds with vanishing pairing amplitudes, named as "domain wall" (DW), where Δ_{ij} gains a phase shift of π. Similarly, due to the existence of DWs which act as nodes for the staggered current and introduce into the SF order parameter a phase shift of π, we refer to the latter as πDSF state.

We consider both original ($q = 0$) and modified ($q = 1$) Gutzwiller factors depending on local hole densities $n_{{\rm h}i}$,

$$g_{ij}^{J} = \frac{4(1-n_{{\rm h}i})(1-n_{{\rm h}j})}{\alpha_{ij} + q[8n_{{\rm h}i}n_{{\rm h}j}\beta_{ij}^{-}(2) + 16\beta_{ij}^{+}(4)]}, \tag{6}$$

$$g_{ij}^{t} = \sqrt{\frac{4n_{{\rm h}i}n_{{\rm h}j}(1-n_{{\rm h}i})(1-n_{{\rm h}j})}{\alpha_{ij} + q[8(1-n_{{\rm h}i}n_{{\rm h}j})|\chi_{ij}|^2 + 16|\chi_{ij}|^4]}}, \tag{7}$$

with $\alpha_{ij} = (1-n_{{\rm h}i}^2)(1-n_{{\rm h}j}^2)$ and $\beta_{ij}^{\pm}(n) = |\Delta_{ij}|^n \pm |\chi_{ij}|^n$. Let us note, however, that the Gutzwiller renormalization scheme becomes substantially more complicated in

the case of inhomogeneous charge distribution as the local density may change before/after projection [17]. As a consequence, Eqs. (6) and (7) may provide only an approximate way of the Gutzwiller projection. Finally, using the unit cell translation symmetry [18], calculations were carried out on a large 256×256 cluster at a low temperature $\beta J = 500$.

The corresponding stripe profiles in both phases shown in Figs. 3 and 4 are clearly a compromise between the superexchange energy E_J and kinetic energy E_t of doped holes. On the one hand, a reduction of the SC or flux order parameters (the latter known to frustrate coherent hole motion [19]) enables a large bond charge hopping $\mathcal{T}_i^y = 2g_{i,i+y}^t \mathrm{Re}(\chi_{i,i+y})$ along the DWs as in the usual stripe scenario [18]. On the other hand, it simultaneously results in the suppression of the AF correlations $\mathcal{S}_i^x = -\frac{3}{2} g_{i,i+x}^J (|\chi_{i,i+x}|^2 + |\Delta_{i,i+x}|^2)$ along the transverse bonds.

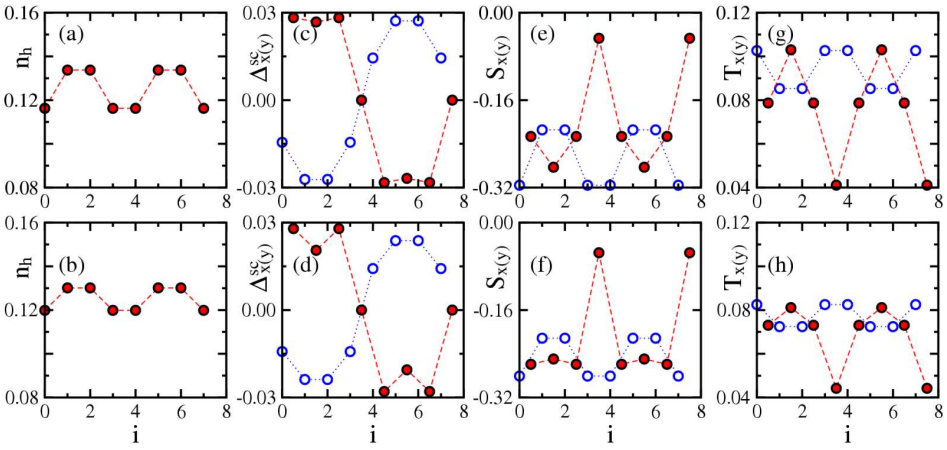

Fig. 3. (a,b) Hole density n_{hi}, (c,d) SC order parameter $\Delta_{i\alpha}^{SC}$, (e,f) spin correlation $\mathcal{S}_i^x$, and (g,h) bond charge $\mathcal{T}_i^y$, found in the πDRVB phase. Top (bottom) parts depict the results obtained using original (modified) Gutzwiller factors; solid (open) circles in parts (c)–(h) correspond to the x (y) direction, respectively.

However, a closer inspection of Figs. 3 and 4 as well as Table indicates that this competition is especially subtle in the πDRVB state. Indeed, instead of increasing hole level in the SC areas in order to reinforce the SC order parameter, the system prefers a more spread out charge distribution, which suggests that the d-wave RVB state is less disposed to phase separation than the SF one where in fact also other charge instabilities have been found [20, 21]. Moreover, as listed in Table, both E_t and E_J are reduced with respect to the uniform d-wave RVB superconductor. In contrast, πDSF phase fully optimizes both energy contributions simply by expelling holes from the regions between the stripes and accommodating them at the DWs. Indeed, a low local doping level strengthens plaquette flux

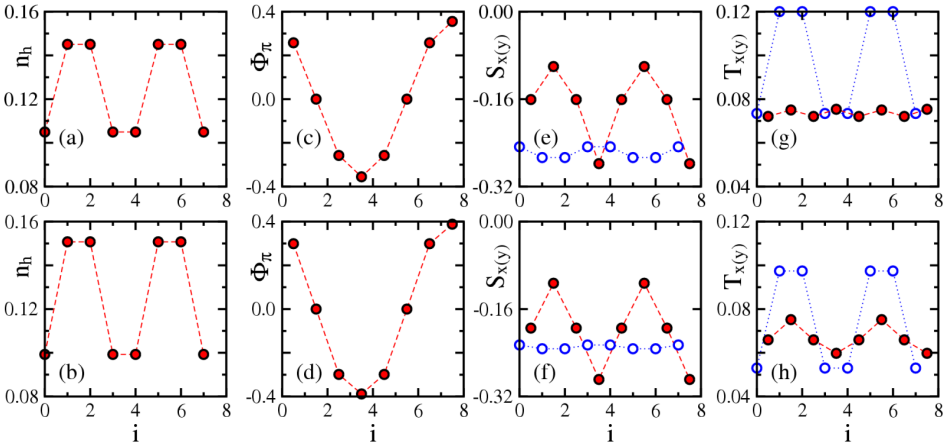

Fig. 4. (a,b) Hole density $n_{\mathrm{h}i}$, (c,d) modulated flux $\Phi_{\pi i}$, (e,f) spin correlation $\mathcal{S}_i^x$, and (g,h) bond charge $\mathcal{T}_i^y$, found in the πDSF phase. Top (bottom) parts depict the results obtained using original (modified) Gutzwiller factors; solid (open) circles in parts (e)–(h) correspond to the x (y) direction, respectively.

which reaches the value $\Phi_{\square} \approx 0.35$ expected for $x \approx 0.1$ (see Fig. 2b). Moreover, the holes accommodated at the DWs enhance locally Gutzwiller factors g_{ij}^t and allow the phase to retain a favorable E_t. Taken together, these two effects are responsible for a much stronger charge modulation of the πDSF phase as compared to its πDRVB counterpart.

TABLE

RMFT kinetic energy E_t, magnetic energy E_J, and free energy F of the locally stable phases: πDSF, SF, πDRVB, and d-wave RVB one at $x = 1/8$.

	Original g_{ij}			Modified g_{ij}		
Phase	E_t/J	E_J/J	F/J	E_t/J	E_J/J	F/J
πDSF	-1.0252	-0.4320	-1.4572	-0.8514	-0.4269	-1.2783
SF	-1.0345	-0.4246	-1.4591	-0.8622	-0.4230	-1.2852
πDRVB	-1.0160	-0.4607	-1.4767	-0.8719	-0.4518	-1.3237
RVB	-1.0232	-0.4838	-1.5070	-0.8863	-0.4784	-1.3647

Unfortunately, the total RMFT energy in both phases differs substantially from the one obtained within the VMC scheme: $E_{\mathrm{DRVB}}/J \approx -1.34$ ($E_{\mathrm{DSF}}/J \approx -1.33$) for the πDRVB (πDSF) phase, respectively [11]. We consider therefore the so-called modified Gutzwiller factors where the effects of the nearest-neighbor correlations χ_{ij} and Δ_{ij} are also included [22]. First of all, one observes that the inclusion of the intersite correlations weakens (strengthens) stripe order in the πDRVB

(πDSF) phase, respectively. Indeed, in both cases the holes are ejected from the regions in between stripes into the DWs defined as nodes of the SC/flux order parameter. Similar tendency towards accommodating the holes at the DWs has also been established in the VMC calculations [23]. Furthermore, while the short--range AF correlations remain either unaltered or they are changed in such a way that E_J remains almost constant, modified Gutzwiller factors mainly renormalize bond charge hopping. As a consequence, the total energy in both phases approaches the one found in the VMC scheme (see Table).

In summary, we believe that our results provide insights into the formation of the recently found bond-centered charge order that coexists with modulated d-wave superconductivity. Moreover, we expect a further enhancement of the proposed valence bond crystal near impurities that break the space group symmetry of the t–J Hamiltonian by producing a modulation in the magnitude of the superexchange coupling [23]. In fact, it has recently been argued that the dopant--induced spatial variation of the atomic levels indeed strengthens locally the AF superexchange interaction [24].

Acknowledgments

The author acknowledges support from the Foundation for Polish Science (FNP), Ministère Français des Affaires Etrangères under Bourse de Recherche, as well as from Polish Ministry of Science and Education under project No. N202 068 32/1481.

References

[1] K.A. Chao, J. Spałek, A.M. Oleś, *J. Phys. C* **10**, L271 (1977); *Phys. Rev. B* **18**, 3453 (1978); F.C. Zhang, T.M. Rice, *ibid.* **37**, 3759 (1988).

[2] S. Sachdev, *Rev. Mod. Phys.* **75**, 913 (2003).

[3] P.W. Anderson, *Science* **235**, 1196 (1987).

[4] F.C. Zhang, C. Gros, T.M. Rice, H. Shiba, *Supercond. Sci. Technol.* **1**, 36 (1988).

[5] S. Sorella, G.B. Martins, F. Becca, C. Gazza, L. Capriotti, A. Parola, E. Dagotto, *Phys. Rev. Lett.* **88**, 117002 (2002).

[6] G. Kotliar, J. Liu, *Phys. Rev. B* **38**, 5142 (1988).

[7] K.-Y. Yang, C.T. Shih, C.P. Chou, S.M. Huang, T.K. Lee, T. Xiang, F.C. Zhang, *Phys. Rev. B* **73**, 224513 (2006).

[8] N.B. Christensen, H.M. Rønnow, J. Mesot, R.A. Ewings, N. Momono, M. Oda, M. Ido, M. Enderle, D.F. McMorrow, A.T. Boothroyd, *Phys. Rev. Lett.* **98**, 197003 (2007); P. Abbamonte, A. Rusydi, S. Smadici, G.D. Gu, G.A. Sawatzky, D.L. Feng, *Nature Phys.* **1**, 155 (2005).

[9] T. Valla, A.V. Fedorov, J. Lee, J.C. Davis, G.D. Gu, *Science* **314**, 1914 (2006).

[10] Y. Kohsaka, C. Taylor, K. Fujita, A. Schmidt, C. Lupien, T. Hanaguri, M. Azuma, M. Takano, H. Eisaki, H. Takagi, S. Uchida, J.C. Davis, *Science* **315**, 1380 (2007); see also J. Zaanen, *ibid.* **315**, 1372 (2007).

[11] M. Raczkowski, M. Capello, D. Poilblanc, R. Frésard, A.M. Oleś, *Phys. Rev. B* **76**, 140505(R) (2007); see also M. Vojta, O. Rösch, *Phys. Rev. B* **77**, 094504 (2008).

[12] I. Affleck, J.B. Marston, *Phys. Rev. B* **37**, R3774 (1988).

[13] D.A. Ivanov, P.A. Lee, X.-G. Wen, *Phys. Rev. Lett.* **84**, 3958 (2000).

[14] P.W. Leung, *Phys. Rev. B* **62**, R6112 (2000).

[15] P. Wróbel, R. Eder, *Phys. Rev. B* **64**, 184504 (2001).

[16] A. Himeda, T. Kato, M. Ogata, *Phys. Rev. Lett.* **88**, 117001 (2002).

[17] B. Edegger, V.N. Muthukumar, C. Gros, *Adv. Phys.* **56**, 927 (2007).

[18] M. Raczkowski, R. Frésard, A.M. Oleś, *Phys. Rev. B* **73**, 174525 (2006); *Europhys. Lett.* **76**, 128 (2006).

[19] D. Poilblanc, Y. Hasegawa, *Phys. Rev. B* **41**, 6989 (1990).

[20] D. Poilblanc, *Phys. Rev. B* **72**, 060508(R) (2005).

[21] M. Raczkowski, D. Poilblanc, R. Frésard, A.M. Oleś, *Phys. Rev. B* **75**, 094505 (2007).

[22] M. Sigrist, T.M. Rice, F.C. Zhang, *Phys. Rev. B* **49**, 12058 (1994).

[23] M.A. Metlitski, S. Sachdev, *Phys. Rev. B* **77**, 054411 (2008).

[24] M.M. Maśka, Ż. Śledź, K. Czajka, M. Mierzejewski, *Phys. Rev. Lett.* **99**, 147006 (2007).